Hindawi
Journal of Chemistry
Volume 2023, Article ID 1399703, 10 pages
https://doi.org/10.1155/2023/1399703

Research Article

Structural, Optical, and Bioactivity Properties of Silver-Doped Zinc Sulfide Nanoparticles Synthesized Using *Plectranthus barbatus* Leaf Extract

Adnan Alnehia,[1,2] **Annas Al-Sharabi**,[2] **A. H. Al-Hammadi**,[1] **Abdel-Basit Al-Odayni**,[3,4] **Waseem Sharaf Saeed**,[3] **and Ali Alrahlah**[3]

[1]*Department of Physics, Faculty of Sciences, Sana'a University, Sana'a, Yemen*
[2]*Department of Physics, Faculty of Applied Sciences, Thamar University, Dhamar 87246, Yemen*
[3]*Engineer Abdullah Bugshan Research Chair for Dental and Oral Rehabilitation, College of Dentistry, King Saud University, Riyadh 11545, Saudi Arabia*
[4]*Department of Chemistry, Faculty of Education, Thamar University, Dhamar 87246, Yemen*

Correspondence should be addressed to Adnan Alnehia; ad.alnehia@su.edu.ye and Abdel-Basit Al-Odayni; aalodayni@ksu.edu.sa

Received 22 March 2023; Revised 16 May 2023; Accepted 18 June 2023; Published 23 June 2023

Academic Editor: Jorge F. Fernandez-Sanchez

Aqueous leaf extract of *Plectranthus barbatus* was used, for the first time, for preparation of (2, 6 mol%) silver (Ag)-doped zinc sulfide nanoparticles (ZnS NPs), acting as a stabilizing and capping agent for NPs' production. The obtained metal oxides were characterized by FTIR, UV-visible, XRD, and SEM methods. The results revealed that 0.02 and 0.06% Ag-doped ZnS had optical bandgaps of 3.20 and 3.03 eV. The XRD evinced the crystalline nature, while the FTIR confirmed the doped structure of the prepared oxides. The bioactivity investigations revealed that the biosynthesized Ag-doped ZnS NPs are more active against *S. aureus* than *E. coli*. Furthermore, the hemolytic tests indicated no potential harm to red blood cells if utilized at a low dose. Such enhanced optical and biological properties of Ag-doped ZnS may promote its prospective use in electronics and as an antibacterial agent.

1. Introduction

Green synthesis of metal sulfide nanoparticles (NPs) is a growing field of nanoscience and nanotechnology. The nanomaterial's size and shape are key factors in its optical, morphological, spectral, structural, and antibacterial properties [1–5]. Zinc sulfide nanoparticles (ZnS NPs) are one of the significant semiconductor materials due to their large bandgap (3.68 eV) and wide exciton binding energy (38 meV) at room temperature (RT) [6–12]. This makes it great for use in many applications. NPs can be produced via chemical and physical routes, which are expensive, hurtful to the environment, and need high energy use. In the literature, the use of plant extracts, microbes, fungi, and enzymes in the synthesis of various metal sulfide NPs has been suggested as a potential ecofriendly substitute for chemical and physical methods [13–18]. However, developing efficient, environment-friendly routes for producing NPs with a certain size, shape, composition, and yield remains challenging.

In this study, the synthesis and subsequence characterization of Ag-doped ZnS NPs by using *Plectranthus barbatus* leaf (PBL) extract are reported for the first time. PBL is a medicinal herb that grows in several countries, such as tropical East Africa, Egypt, Brazil, India, Yemen, and Saudi Arabia. According to the literature, PBL can serve as an antibacterial agent [19, 20]. Furthermore, the plant is also safe for conventional usage and is used to treat a variety of disorders, including seizures [21]. Phytochemical studies revealed the presence of various phytocompounds in the plant, of which forskolin is the dominant and most active against seizures. The plant leaf aqueous

extract has been reported to predominantly contain terpenoids, saponins, tannins, alkaloids, and essential oils [22].

Hence, the study describes the synthesis of 2% and 6% Ag-doped ZnS NPs using *Plectranthus barbatus* leaf extract. To our knowledge, the biosynthesis of Ag-doped ZnS NPs using PBL extract and their antimicrobial activity is poorly documented. To this end, the primary objective of this work is to produce Ag-doped ZnS NPs using the PBL extract. The influence of Ag doping on the properties of ZnS is also investigated using various characterization tools, including XRD, SEM, FTIR, and UV-visible. Furthermore, their antibacterial and hemolytic activities were tested.

2. Materials and Methods

2.1. Materials. Zinc nitrate hexahydrate ($Zn(NO_3)_2{\cdot}6H_2O$; 98.5%), silver nitrate ($AgNO_3$; 98%), sodium sulfide (Na_2S; 97%), and ethanol (EtOH; 96) were purchased from BDH Chemical Ltd. (Pool, England, UK). The *Escherichia coli* (*E. coli*) and *Staphylococcus aureus* (*S. aureus*) test bacteria were kind gifts from Alfa Medical Laboratory, Thamar city, Yemen. Mueller–Hinton Agar (MHA) was procured from Sigma-Aldrich (Darmstadt, Germany). Distilled water (dH_2O) was used wherever required. Fresh leaves of *Plectranthus barbatus* (PBL) were collected, during the summer season of 2021, from Anis district, Thamar governorate, Yemen.

2.2. Preparation of Aqueous Leaf Extract. *Plectranthus barbatus* leaves were washed with tap water, then dried and washed using dH_2O and ethanol to remove dust particles. The leaves were cut into small pieces and crushed with mortar and pestle into a paste. To synthesize the aqueous extract of *Plectranthus barbatus* leaves, 16 g of the leaves' paste were mixed with 250 mL dH_2O. The mixture was stirred on a magnetic stirrer at 25°C for 90 minutes until the color of the solution changed from colorless to brown. The extract was filtered and utilized to synthesize Ag-doped ZnS [23–25].

2.3. Synthesis of Ag-Doped ZnS NPs. In the first, 25 mL of leaf extract was taken and poured into a beaker with a volume of 100 mL. The beaker was put on a magnetic stirrer. Then, 8.18 g of $Zn(NO_3)_2{\cdot}6H_2O$ was added to the solution at 23 ± 2°C with constant stirring. Also, 2.14 g of Na_2S was mixed in 25 mL of aqueous leaf extract at 23 ± 2°C. Both solutions were mixed in a new beaker with constant stirring at RT for 60 min, and 2% Ag was added during mixing. The mixture was converted to a brown-colored solution. The obtained precipitate was filtered, washed sequentially, three times with dH_2O and EtOH and dried at RT for 24 h. After that, the product was collected in a crucible and dried in an oven at 100°C for 90 mins. The brown-colored powder was ground using a mortar and pestle. Finally, nanopowder was stored for further characterization [24, 26]. Similarly, the same procedures were repeated with doping ZnS NPs with 0.06 Ag. The overall experiments are schematically shown in Figure 1.

2.4. Antibacterial Test. The antibacterial effect of the synthesized samples was executed for *E. coli* (Gram negative) and *S. aureus* (Gram positive) bacteria using the disc diffusion technique [27–29]. The concentrations of 67, 134, and 201 mg/mL of the synthesized NPs were taken for the antibacterial check. After incubation at 35–37°C for 24 h, the zones of inhibition (ZOI) were measured.

2.5. Characterization Techniques. The structural properties and phase identification of Ag-doped ZnS NPs were analyzed using an X-ray diffractometer (Shimadzu EDX-720, China) with Cu K_α radiation ($\lambda = 0.154$ nm). The optical properties were studied using a UV-vis spectrophotometer (Hitachi U3900) with the software of Varian Cary 50. The FTIR spectrum was recorded on a Nicolet iS10 from Thermo Scientific (Madison, WI, USA, USA). The surface morphology imaging was performed on a JSM-6360 LV SEM (Jeol Ltd., Tokyo, Japan).

3. Results and Discussion

3.1. XRD Analysis. The crystal structures of prepared 2% and 6% Ag-doped ZnS NPs were investigated via XRD, as shown in Figure 2. As depicted in Figure 2, three prominent diffraction peaks were indexed for zinc sulfide displays, corresponding to the (111), (220), and (311) of cubic ZnS (JCPDS Card, No. 05-0566). In addition, a new diffraction peak was indexed. This characteristic diffraction peak corresponds to hexagonal Zn (JCPDS Card No. 04-0831). The XRD results emphasize the formation of ZnS-Zn nanoparticles. After doping of ZnS-Zn NPs with 6% Ag ions, two new peaks were observed, and thus indexed for Ag dopant and assigned to the (111) and (200) of cubic Ag (JCPDS Card, No. 04-0783). The XRD peaks for Ag-ZnS demonstrate the formation of clear distinct phases for Ag, ZnS, and Zn. The crystallite size D (nm) and the average dislocation density (δ) for all the synthesized materials were estimated using the Scherer formula $D = (0.9\lambda/\beta\cos\theta)$ [30, 31] and $\delta = 1/D^2$ [32], respectively. The microstrain (ε) was computed using the equation $\varepsilon = \beta\cos\theta/4$, where β is the full width at half maximum, $\lambda = 0.154$ nm, and θ is Bragg's diffraction angle, and Stacking fault (SF) was calculated by the equation $SF = [\mathbf{2}\pi^2/\mathbf{45}\,(\mathbf{3}\tan\theta)^{\mathbf{0.5}}]\beta$ [33, 34]. The results are summarized in Table 1.

3.2. SEM Analysis. The morphology of the synthesized NPs was studied via SEM device. Figure 3 shows an SEM micrograph of 6% Ag-doped ZnS NPs. The SEM image reveals irregularly shaped NPs, existing in an agglomerated structure with a stone-like profile.

3.3. UV-Vis Analysis. The absorption spectra of 2% and 6% Ag-doped ZnS NPs are shown in Figure 4, in the wavelength (λ) range of 200–800 nm. It displayed a sharp decrease in

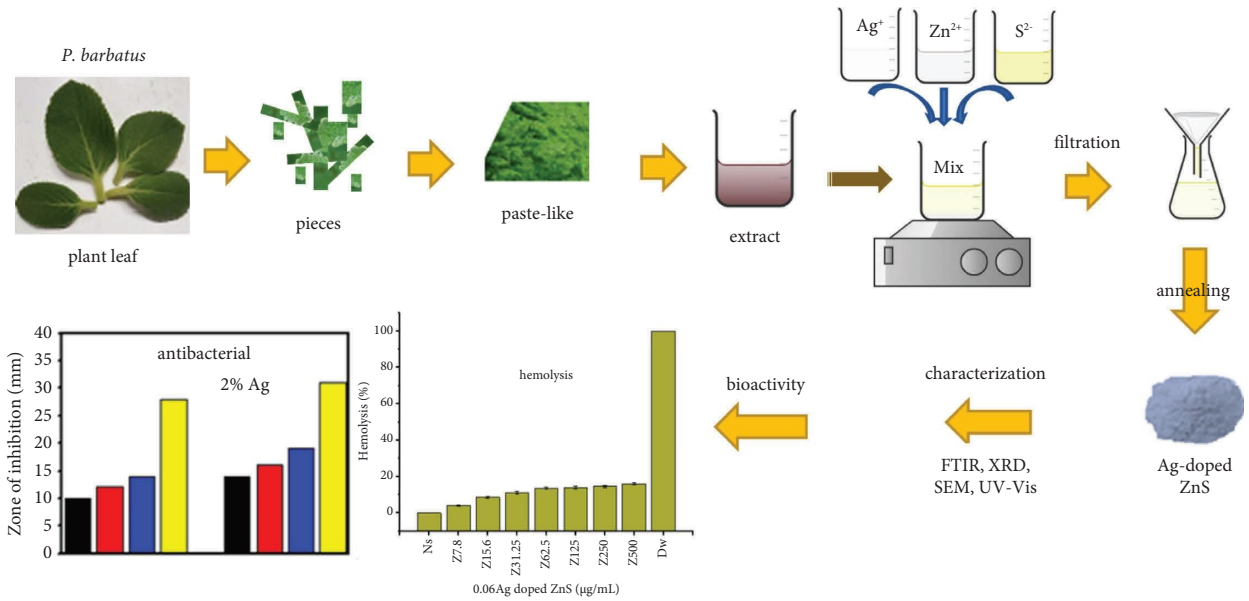

Figure 1: Flow steps for the green synthesis of Ag-doped ZnS NPs using *Plectranthus barbatus* leaves' extract, characterization, and antibacterial activity.

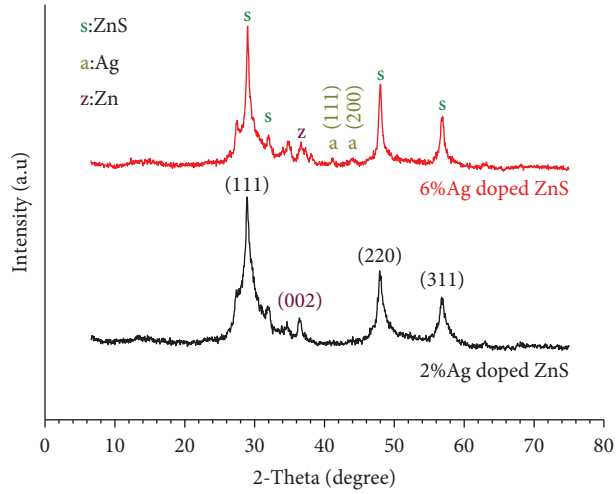

Figure 2: XRD pattern of 2% and 6% Ag-doped ZnS NPs.

Table 1: Structural parameters of Ag-doped ZnS NPs.

Sample	2-theta ($2\theta^{\circ}$)	(hkl)	FWHM (β)	Crystallite size (D, nm)	Average (D, nm)	Average dislocation density (lines/m^2) $*$ 10^{16}	Microstrain (ε)	SF
2% Ag-doped ZnS	29.06	(111)	3.109	2.639	4.419	5.120	0.0131	0.0269
	48.09	(220)	1.753	4.962			0.0069	0.0115
	56.89	(311)	1.597	5.657			0.0061	0.0095
6% Ag-doped ZnS	29.06	(111)	2.669	3.075	8.402	1.416	0.0112	0.0231
	48.01	(220)	0.751	11.58			0.0029	0.0049
	56.86	(311)	0.856	10.55			0.0032	0.0051

optical absorbance with increasing the λ up to 300 nm. Above this range, the optical absorbance was nearly constant. According to the figure, the absorbance is higher for 2% than 6% Ag-doped ZnS NPs.

The coefficient of absorption (α) was evaluated using the Beer–Lambert equation [6, 35]. Figure 5(a) displays the α as a function of incident photon energy ($h\nu$). The α increased with increasing incident photon energy ($h\nu$) for the prepared

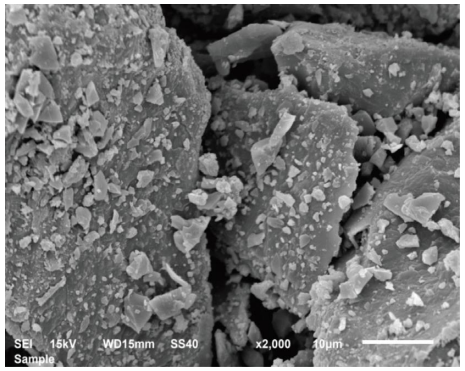

Figure 3: SEM image of 6% Ag-doped ZnS NPs.

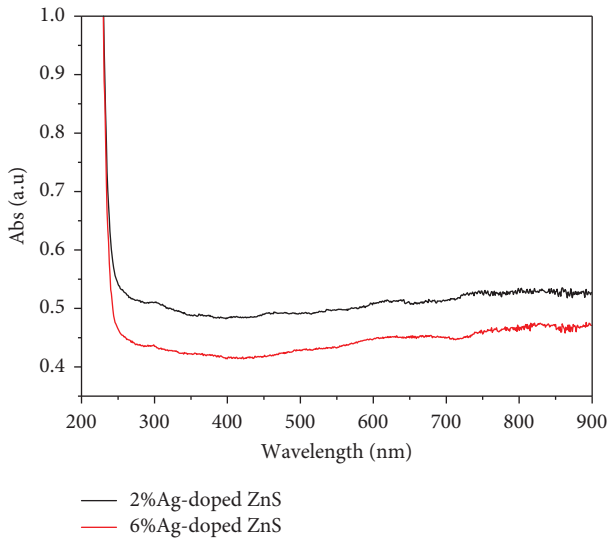

Figure 4: Absorbance spectra of 2% Ag-doped ZnS and 6% Ag-doped ZnS NPs.

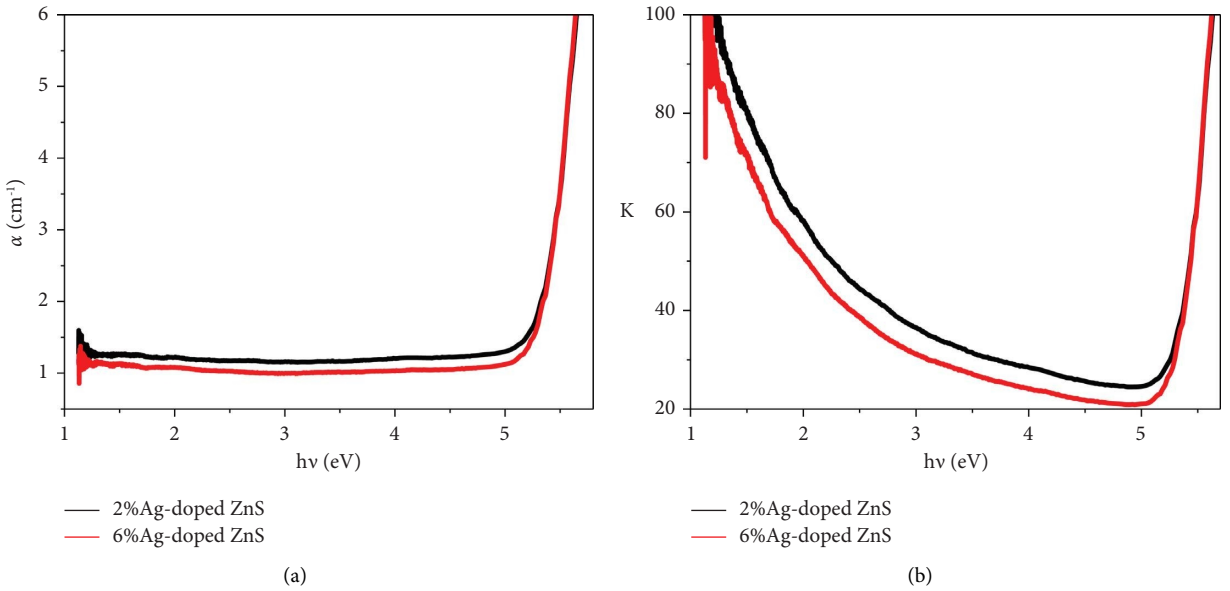

Figure 5: (a) Absorption coefficient (α) and (b) extinction coefficient (k) of 2% Ag-doped ZnS and 6% Ag-doped ZnS NPs.

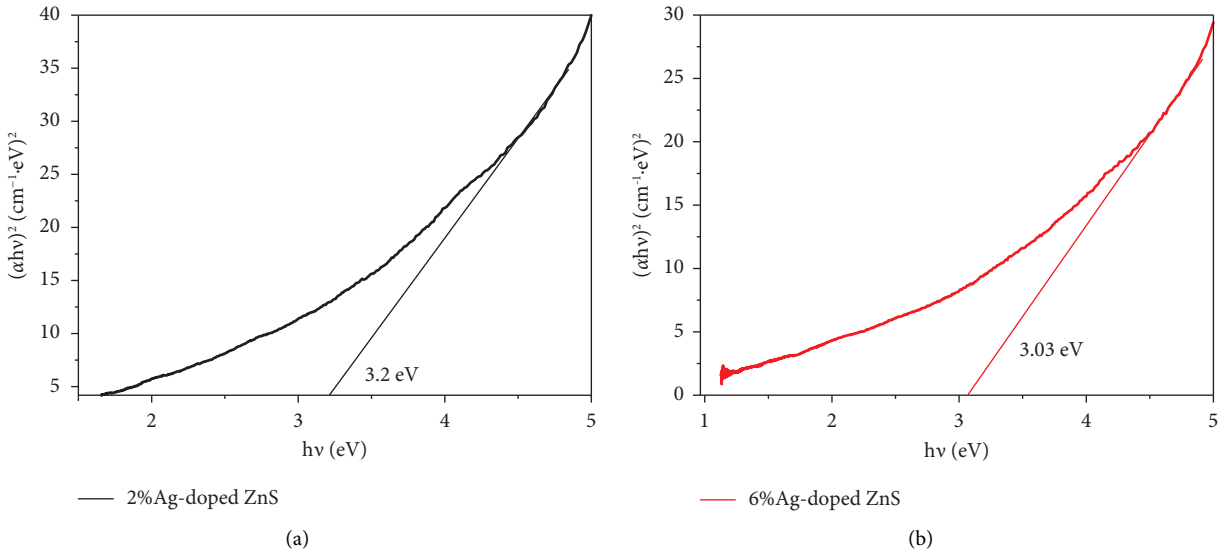

Figure 6: The optical band gap energy (E_g) of (a) 2% Ag-doped ZnS and (b) 6% Ag-doped ZnS NPs.

materials. The coefficient of extinction (k) was evaluated using the equation $k = (\alpha\lambda/4\pi)$ [35, 36]. Figure 5(b) displays the k as a function of incident photon energy ($h\nu$) for the investigated materials. It is obvious that the k decreased as incident photon energy increased and that, up to a certain point after that, the k dramatically increased in response to an increase in photon energy. The optical bandgap energy (E_g) of the synthesized samples can be calculated by Tauc's method [34, 37, 38]. The computed E_g values of Ag (0.02 and 0.06)-doped ZnS NPs were 3.52, 3.20, and 3.03 eV, respectively. Figures 6(a) and 6(b) illustrate the evaluated E_g for the synthesized NPs. The E_g decreases as dopant concentration increases due to the interaction between ZnS and Ag ions. Also, the reduction in the energy gap may be due to the creation of some defects in the ZnS NPs.

3.4. FTIR Analysis. Figure 7 displays the ATR-FTIR spectrum of the prepared 0.06 Ag-doped ZnS NPs. The FTIR is a helpful tool for identifying the functional groups present on the material surface [39, 40]. Here, the spectrum of 0.06 Ag-doped ZnS NPs was listed in the FTIR range of 600–4000 cm^{-1} [41]. Thus, the broadband at 3280 cm^{-1} is due to the stretching vibration of various OH groups, v (OH), involving Zn-OH and water-OH of both free and H-bonding. The peaks at 1100, 960, and 840 cm^{-1} can be attributed to the stretching bands of NO_3^{-1} and asymmetric and symmetric stretching of C-O [40, 42], respectively, in the extract agents that drove the NPs' production.

As it is reported, the *Plectranthus barbatus* plant is rich in forskolin, a labdane diterpenoid compound [21]. Hence, its leaf aqueous extract has been reported to contain terpenoids, saponins, tannins, alkaloids, and essential oils [22]. These compounds are associated with specific functional groups that could be involved in the production of NPs [43, 44]. As depicted in Figure 8, the phytocompounds serve as capping and stabilizing agents during the biosynthesis of NPs [43]. In this case, plant-based compounds such as

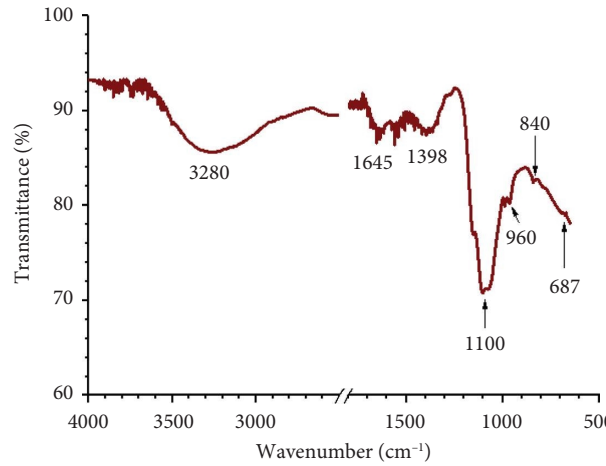

Figure 7: FTIR spectra of 6% Ag-doped ZnS NPs.

amino acids and terpenoids (as representatives for the target phytocompounds in the *PBL* extract [29, 45, 46]) can stabilize sulfide and metal (i.e., Zn^{2+}, S^{2-}, and Ag^{+}) ions, respectively, which are further hydrolyzed to the corresponding NPs.

3.5. Antibacterial Activity. The antibacterial activity of the as-synthesized Ag-doped ZnS NPs was investigated against *S. aureus* and *E. coli* bacterial strains to determine their utility as potential materials for biological applications. Figure 9(a) depicts selected images of antibacterial Petri plates, and the results are presented in the histogram in Figure 9(b). The results (Table 2) revealed that the antibacterial effect of 2% is less than that of 6% Ag-doped ZnS NPs. The variation between the antibacterial effects of the bacteria strains can be interpreted via the composition of chemical and diverse structure of every cell surface. The high antibacterial activities are because of the increased ability of

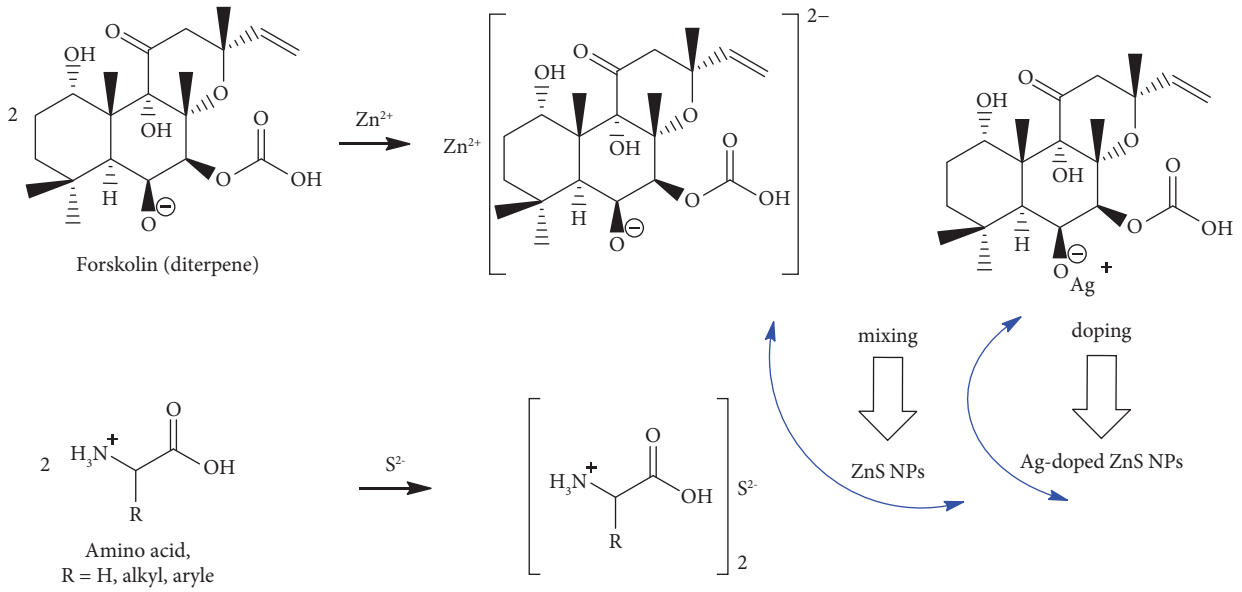

Figure 8: Schematic illustration of the proposed mechanism for biosynthesis of ZnS and Ag-doped ZnS using *Plectranthus barbatus*-based biogenic compounds.

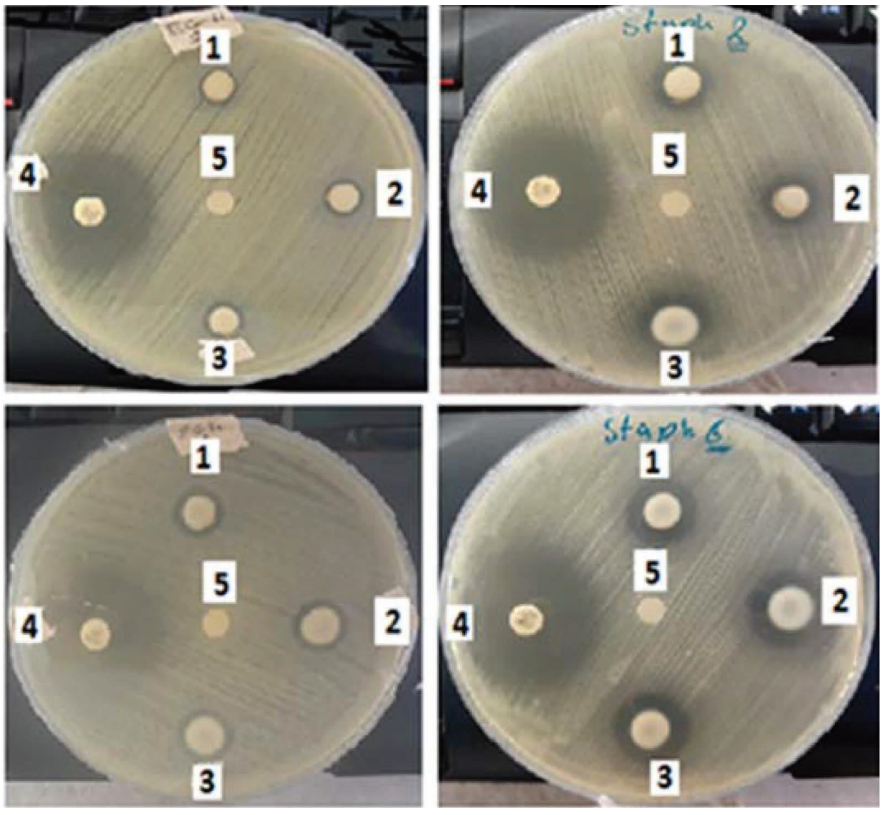

(a)

Figure 9: Continued.

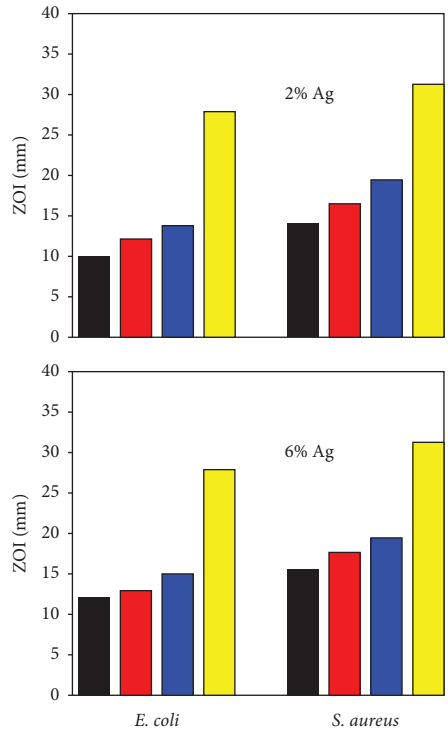

(b)

Figure 9: (a) Antibacterial activity of 2% Ag and 6% Ag-doped ZnS NPs against *E. coli* and *S. aureus*: (1) 67 mg/mL (2) 134 mg/mL, (3) 201 mg/mL per disc, (4) distilled water (negative control) and (4) azithromycin antibiotics (positive control). (b) Histogram illustration for the corresponding zone of inhibition (ZOI).

Table 2: Antibacterial activity of prepared 6% Ag-doped ZnS NPs.

Samples	Bacteria	ZOI (diameter in mm) at various concentrations (mg/mL)			
		67 mg/mL	134 mg/mL	201 mg/mL	Control (azithromycin)
2% Ag-doped ZnS	*S. aureus*	14	16	19	31
	E. coli	10	12	14	28
6% Ag-doped ZnS	*S. aureus*	16	18	20	31
	E. coli	12	13	15	28

the fabricated NPs to generate reactive oxygen species (ROS) [4, 47–50].

Typically, there are more than one suggested mechanism, and the destructive action can undergo one or more of them [28, 51, 52]. Of these mechanisms, there are (i) direct interaction of bioactive agent with the microorganism surface leading to membrane damaging, then component leakage, and finally functionality loss; (ii) penetration of released ions which inhibit several essential cell activities, resulting in cell death; and (iii) generation of ROS which, at the end, cause cell damage as a result of catalytic degradation.

3.6. Hemolytic Activity. Hemolytic activity against erythrocytes using a *Plectranthus barbatus* leaf extract mediated 0.06 Ag-doped ZnS NPs was estimated over a concentration range of 7.8–500 μg/mL. Experimental procedures were performed as previously described [53] with a few adjustments. In brief, 5 mL of blood was taken from a healthy female volunteer (22 years old, O-positive (O^+) blood group). The blood samples were conveyed into an EDTA tube; then, RBCs were isolated using a typical procedure described elsewhere. The EDTA-blood suspension was centrifuged at 4000 rpm for 10 min, decanting the supernatant, and the pellets were adequately washed with 0.9% normal saline (NS) solution. The test erythrocyte suspension was diluted to 2% cells, while check samples of 0.06 Ag-doped ZnS NPs were synthesized as 7.8–500 μg/mL in NS. Experimentally, 0.5 mL of the cell suspension was mixed with 0.5 mL of each test sample and immediately incubated at 37°C for 60 min. After that, solutions were centrifuged at 4000 rpm for 10 min to remove cell depression, and the supernatant containing free hemoglobin was photometrically measured at 540 nm. Sterile NS and DW were used as minimal and maximal hemolytic controls and experimentally treated as test samples. The hemolytic percentage was computed based on the following equation [53, 54]:

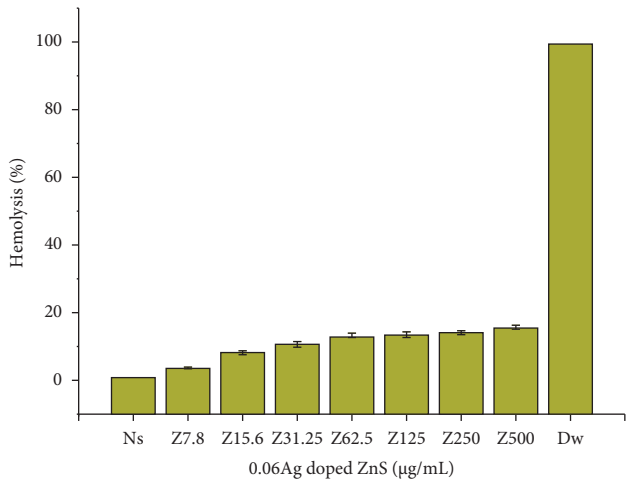

FIGURE 10: Hemolytic activity of 0.06 Ag-doped ZnS NPs at different concentrations (7.8–500 μg/mL), NS (negative control), and DW (positive control).

$$\text{Hemolysis\%} = \left(\frac{A_S - A_N}{A_P - A_N}\right) \times 100, \quad (1)$$

where A_S, A_N, and A_P are the absorbance of the NPs (the sample), NS (negative control), and DW (positive control), respectively.

Figure 10 displays the average hemolytic activity from two independent experiments. Cytotoxicity of 0.06 Ag-doped ZnS NPs was observed (15.97%) at the higher doses of 500 μg/mL, while no hemolysis was detected at a concentration of 7.8 μg/mL. The results recorded in Figure 10 display the less cytotoxic influence of 0.06 Ag-doped ZnS NPs on isolated RBCs. These results strongly agree with previous studies by Muhammad et al. [29, 55].

4. Conclusions

This paper shows that 2% and 6% Ag-doped ZnS NPs have successfully prepared using the green route. The XRD and FTIR data proved the crystallite structure of the prepared metal oxides. The UV-vis spectra revealed that the optical bandgap decreased with increasing Ag content. The antibacterial effect of 2% Ag-doped ZnS was less than that of 6% Ag-doped ZnS NPs. Furthermore, the effect was found to be less on Gram negative than on Gram positive. The hemolysis study indicated no potential harm due to Ag-ZnS to red blood cells if used in low doses. Our results showed that Ag-ZnS NPs produced from *Plectranthus barbatus* leaf extract might be a safe and efficacious resource for antibiotic development.

Data Availability

The data used to support the findings of this study are included within the article.

Conflicts of Interest

The authors declare that they have no conflicts of interest.

Acknowledgments

The authors extend their appreciation to the Deputyship for Research and Innovation, Ministry of Education in Saudi Arabia for funding this research (IFKSURC-1-1901).

References

[1] K. Saravanadevi, M. Kavitha, P. Karpagavinayagam, K. Saminathan, and C. Vedhi, "Biosynthesis of ZnO and Ag doped ZnO nanoparticles from Vitis vinifera leaf for antibacterial, photocatalytic application," *Materials Today: Proceedings*, vol. 48, pp. 352–356, 2022.

[2] J. Dhatwalia, A. Kumari, A. Chauhan et al., "Rubus ellipticus Sm. Fruit extract mediated zinc oxide nanoparticles: a green approach for dye degradation and biomedical applications," *Materials*, vol. 15, no. 10, p. 3470, 2022.

[3] M. H. Morowvat, K. Kazemi, M. A. Jaberi, A. Amini, and A. Gholami, "Biosynthesis and antimicrobial evaluation of zinc oxide nanoparticles using chlorella vulgaris biomass against multidrug-resistant pathogens," *Materials*, vol. 16, no. 2, p. 842, 2023.

[4] A. Alnehia, A. Al-Sharabi, A. H. Al-Hammadi, A.-B. Al-Odayni, S. A. Alramadhan, and R. M. Alodeni, "Phyto-mediated synthesis of silver-doped zinc oxide nanoparticles from Plectranthus barbatus leaf extract: optical, morphological, and antibacterial properties," *Biomass Conversion and Biorefinery*, 2023.

[5] S. Slathia, T. Gupta, and R. P. Chauhan, "Green synthesis of Ag–ZnO nanocomposite using Azadirachta indica leaf extract exhibiting excellent optical and electrical properties," *Physica B: Condensed Matter*, vol. 621, Article ID 413287, 2021.

[6] A. Al-Sharabi, A. Alnehia, A. H. Al-Hammadi, K. A. Alhumaidha, and A. Al-Osta, "The effect of Nigella sativa seed extract concentration on crystal structure, band gap and antibacterial activity of ZnS-NPs prepared by green route," *Journal of Materials Science: Materials in Electronics*, vol. 33, no. 26, pp. 20812–20822, 2022.

[7] A. H. Al-Hammadi, A. Al-Sharabi, and A. Alnehia, "Green and chemically prepared zinc sulfide nanoparticles: a comparative study," *Sana'a University Journal of Applied Sciences and Technology*, vol. 1, pp. 70–77, 2023.

[8] J. K. Salem, T. M. Hammad, S. Kuhn et al., "Structural and optical properties of Co-doped ZnS nanoparticles synthesized by a capping agent," *Journal of Materials Science: Materials in Electronics*, vol. 25, no. 5, pp. 2177–2182, 2014.

[9] S. Horoz, Q. Dai, F. S. Maloney et al., "Absorption induced by Mn doping of ZnS for improved sensitized quantum-dot solar cells," *Physical Review Applied*, vol. 3, no. 2, Article ID 024011, 2015.

[10] B. Ayim-Otu, M. Kuncan, O. Şahin, and S. Horoz, "Synthesis and photovoltaic application of ZnS:Cu (3%) nanoparticles," *Journal of the Australian Ceramic Society*, vol. 56, no. 2, pp. 639–643, 2019.

[11] B. Poornaprakash, P. T. Poojitha, U. Chalapathi, K. Subramanyam, and S.-H. Park, "Synthesis, structural, optical, and magnetic properties of Co doped, Sm doped and Co+Sm co-doped ZnS nanoparticles," *Physica E: Low-Dimensional Systems and Nanostructures*, vol. 83, pp. 180–185, 2016.

[12] D. Amaranatha Reddy, A. Divya, G. Murali, R. P. Vijayalakshmi, and B. K. Reddy, "Synthesis and optical properties of Cr doped ZnS nanoparticles capped by 2-

mercaptoethanol," *Physica B: Condensed Matter*, vol. 406, no. 10, pp. 1944–1949, 2011.

[13] P. C. M. dos Santos, L. M. R. da Silva, F. E. A. Magalhaes, F. E. T. Cunha, M. J. G. Ferreira, and E. A. T. de Figueiredo, "Garlic (Allium sativum L.) peel extracts: from industrial by-product to food additive," *Applied Food Research*, vol. 2, Article ID 100186, 2022.

[14] S. Munyai, L. M. Mahlaule-Glory, and N. C. Hintsho-Mbita, "Green synthesis of Zinc sulphide (ZnS) nanostructures using S. frutescences plant extract for photocatalytic degradation of dyes and antibiotics," *Materials Research Express*, vol. 9, no. 1, Article ID 015001, 2022.

[15] H. Q. Alijani, S. Pourseyedi, M. Torkzadeh-Mahani, and M. Khatami, "Green Synthesis of Zinc sulfide (ZnS) Nanoparticles using Stevia rebaudiana Bertoni and evaluation of its cytotoxic properties," *Journal of Molecular Structure*, vol. 1175, pp. 214–218, 2019.

[16] I. Johnson and H. J. Prabu, "Greener cum chemical synthesis and characterization of Mg doped ZnS nanoparticles and their engineering band gap performance," *Journal of Engineering Research and Application*, vol. 5, pp. 99–105, 2015.

[17] D. Hassan, A. T. Khalil, J. Saleem et al., "Biosynthesis of pure hematite phase magnetic iron oxide nanoparticles using floral extracts of Callistemon viminalis (bottlebrush): their physical properties and novel biological applications," *Artificial Cells, Nanomedicine, and Biotechnology*, vol. 46, pp. 693–707, 2018.

[18] A. C. Nwanya, L. C. Razanamahandry, A. Bashir et al., "Industrial textile effluent treatment and antibacterial effectiveness of Zea mays L. Dry husk mediated bio-synthesized copper oxide nanoparticles," *Journal of Hazardous Materials*, vol. 375, pp. 281–289, 2019.

[19] W. A. de Almeida, I. C. V. Nova, J. D. S. Nascimento et al., "Effects of Plectranthus barbatus leaf extract on survival, digestive proteases, midgut morphophysiology and gut microbiota homeostasis of aedes aegypti larvae," *South African Journal of Botany*, vol. 141, pp. 116–125, 2021.

[20] N. L. Figueiredo, S. R. M. de Aguiar, P. L. Falé, L. Ascensão, M. L. M. Serralheiro, and A. R. L. Lino, "The inhibitory effect of Plectranthus barbatus and Plectranthus ecklonii leaves on the viability, glucosyltransferase activity and biofilm formation of Streptococcus sobrinus and Streptococcus mutans," *Food Chemistry*, vol. 119, no. 2, pp. 664–668, 2010.

[21] L. C. Borges Fernandes, C. Campos Câmara, and B. Soto-Blanco, "Anticonvulsant activity of extracts of Plectranthus barbatus leaves in mice," *Evidence-based Complementary and Alternative Medicine*, vol. 2012, Article ID 860153, 4 pages, 2012.

[22] J. O. Ezeonwumelu, G. N. Kawooya, A. G. Okoruwa et al., "Phytochemical screening, toxicity, analgesic and anti-pyretic studies of aqueous leaf extract of Plectranthus barbatus [andrews. Engl.] in rats," *Pharmacology & Pharmacy*, vol. 10, no. 4, pp. 205–221, 2019.

[23] M. M. Khan, M. H. Harunsani, A. L. Tan, M. Hojamberdiev, Y. A. Poi, and N. Ahmad, "Antibacterial studies of ZnO and Cu-doped ZnO nanoparticles synthesized using aqueous leaf extractof stachytarpheta jamaicensis," *BioNanoScience*, vol. 10, no. 4, pp. 1037–1048, 2020.

[24] M. M. Khan, M. H. Harunsani, A. L. Tan, M. Hojamberdiev, S. Azamay, and N. Ahmad, "Antibacterial activities of zinc oxide and Mn-doped zinc oxide synthesized using melastoma malabathricum (L.) leaf extract," *Bioprocess and Biosystems Engineering*, vol. 43, no. 8, pp. 1499–1508, 2020.

[25] T. S. Aldeen, H. E. Ahmed Mohamed, and M. Maaza, "ZnO nanoparticles prepared via a green synthesis approach: physical properties, photocatalytic and antibacterial activity," *Journal of Physics and Chemistry of Solids*, vol. 160, Article ID 110313, 2022.

[26] A. Rahman, M. H. Harunsani, A. L. Tan, N. Ahmad, M. Hojamberdiev, and M. M. Khan, "Effect of Mg doping ZnO fabricated using aqueous leaf extract of Ziziphus mauritiana Lam. for antioxidant and antibacterial studies," *Bioprocess and Biosystems Engineering*, vol. 44, 2021.

[27] M. S. Nadeem, T. Munawar, F. Mukhtar, M. Naveed ur Rahman, M. Riaz, and F. Iqbal, "Enhancement in the photocatalytic and antimicrobial properties of ZnO nanoparticles by structural variations and energy bandgap tuning through Fe and Co co-doping," *Ceramics International*, vol. 47, no. 8, pp. 11109–11121, 2021.

[28] M. Aklilu and T. Aderaw, "Khat (catha edulis) leaf extract-based zinc oxide nanoparticles and evaluation of their antibacterial activity," *Journal of Nanomaterials*, vol. 2022, Article ID 4048120, 10 pages, 2022.

[29] A. Alnehia, A.-B. Al-Odayni, A. H. Al-Hammadi et al., "Garlic extract–mediated synthesis of ZnSNanoparticles: structural, optical, antibacterial and hemolysis studies," *Journal of Nanomaterials*, vol. 2023, Article ID 8200912, 9 pages, 2023.

[30] F. Mukhtar, T. Munawar, M. S. Nadeem, M. N. U. Rehman, M. Riaz, and F. Iqbal, "Dual S-scheme heterojunction ZnO–V_2O_5–WO nanocomposite with enhanced photocatalytic and antimicrobial activity," *Materials Chemistry and Physics*, vol. 263, Article ID 124372, 2021.

[31] A. M. Abdulwahab, E. A. Al-Mahdi, A. Al-Osta, and A. A. Qaid, "Structural, optical and electrical properties of CuSCN nano-powders doped with Li for optoelectronic applications," *Chinese Journal of Physics*, vol. 73, pp. 479–492, 2021.

[32] K. Karthik, S. Dhanuskodi, C. Gobinath, S. Prabukumar, and S. Sivaramakrishnan, "Ultrasonic-assisted CdO–MgO nanocomposite for multifunctional applications," *Materials Technology*, vol. 34, no. 7, pp. 403–414, 2019.

[33] A. Rahman, M. H. Harunsani, A. L. Tan, N. Ahmad, B.-K. Min, and M. M. Khan, "Influence of Mg and Cu dual-doping on phytogenic synthesized ZnO for light induced antibacterial and radical scavenging activities," *Materials Science in Semiconductor Processing*, vol. 128, Article ID 105761, 2021.

[34] A. B. Alwany, G. M. Youssef, E. E. Saleh, O. M. Samir, M. A. Algradee, and A. Alnehia, "Structural, optical and radiation shielding properties of ZnS nanoparticles QDs," *Optik*, vol. 260, Article ID 169124, 2022.

[35] A. Alnehia, A. H. Al-Hammadi, A. Al-Sharabi, and H. Alnahari, "Optical, structural and morphological properties of ZnO and Fe+3 doped ZnO-NPs prepared by Foeniculum vulgare extract as capping agent for optoelectronic applications," *Inorganic Chemistry Communications*, vol. 143, Article ID 109699, 2022.

[36] A. Al-Osta, A. Alnehia, A. A. Qaid, H. T. Al-Ahsab, and A. Al-Sharabi, "Structural, morphological and optical properties of Cr doped ZnS nanoparticles prepared without any capping agent," *Optik*, vol. 214, Article ID 164831, 2020.

[37] A. Rajeh, H. M. Ragab, and M. M. Abutalib, "Co doped ZnO reinforced PEMA/PMMA composite: structural, thermal, dielectric and electrical properties for electrochemical applications," *Journal of Molecular Structure*, vol. 1217, Article ID 128447, 2020.

[38] J. Sharma, A. Gupta, and O. P. Pandey, "Effect of Zr doping and aging on optical and photocatalytic properties of ZnS

nanopowder," *Ceramics International*, vol. 45, no. 11, pp. 13671–13678, 2019.

[39] D. Letsholathebe, F. Thema, K. Mphale, K. Maabong, and C. Maria Magdalane, "Green synthesis of ZnO doped Moringa oleifera leaf extract using Titon yellow dye for photocatalytic applications," *Materials Today: Proceedings*, vol. 36, pp. 475–479, 2021.

[40] W. Ahmad and D. Kalra, "Green synthesis, characterization and anti microbial activities of ZnO nanoparticles using Euphorbia hirta leaf extract," *Journal of King Saud University Science*, vol. 32, no. 4, pp. 2358–2364, 2020.

[41] T. Gutul, E. Rusu, N. Condur, V. Ursaki, E. Goncearenco, and P. Vlazan, "Preparation of poly (N-vinylpyrrolidone)-stabilized ZnO colloid nanoparticles," *Beilstein Journal of Nanotechnology*, vol. 5, pp. 402–406, 2014.

[42] D. Saravanakkumar, S. Sivaranjani, M. Umamaheswari, S. Pandiarajan, and B. Ravikumar, "Green synthesis of ZnO nanoparticles using Trachyspermum ammi seed extract for antibacterial investigation," *Der Pharma Chemica*, vol. 8, pp. 173–180, 2016.

[43] N. Matinise, X. Fuku, K. Kaviyarasu, N. Mayedwa, and M. Maaza, "ZnO nanoparticles via Moringa oleifera green synthesis: physical properties & mechanism of formation," *Applied Surface Science*, vol. 406, pp. 339–347, 2017.

[44] P. Belle Ebanda Kedi, F. Eya'ane Meva, L. Kotsedi et al., "Eco-friendly synthesis, characterization, in vitro and in vivo anti-inflammatory activity of silver nanoparticle-mediated Selaginella myosurus aqueous extract," *International Journal of Nanomedicine*, vol. 13, pp. 8537–8548, 2018.

[45] M. Sharma, H. Bassi, P. Chauhan et al., "Inhibition of the bacterial growth as a consequence of synergism of Ag and ZnO: Calendula officinalis mediated green approach for nanoparticles and impact of altitude," *Inorganic Chemistry Communications*, vol. 136, Article ID 109131, 2022.

[46] A. Al-Sharabi, K. S. Sada'a, A. Al-Osta, and R. Abd-Shukor, "Structure, optical properties and antimicrobial activities of MgO–Bi2– x Cr x O3 nanocomposites prepared via solvent-deficient method," *Scientific Reports*, vol. 12, no. 1, Article ID 10647, 2022.

[47] A. Rahman, M. H. Harunsani, A. L. Tan, N. Ahmad, and M. M. Khan, "Antioxidant and antibacterial studies of phytogenic fabricated ZnO using aqueous leaf extract of Ziziphus mauritiana Lam," *Chemical Papers*, vol. 75, no. 7, pp. 3295–3308, 2021.

[48] A. Dhupar, S. Kumar, H. S. Tuli, A. K. Sharma, V. Sharma, and J. K. Sharma, "In-doped ZnS nanoparticles: structural, morphological, optical and antibacterial properties," *Applied Physics A*, vol. 127, no. 4, pp. 263–274, 2021.

[49] S. O. Aisida, K. Ugwu, P. A. Akpa et al., "Biosynthesis of silver nanoparticles using bitter leave (Veronica amygdalina) for antibacterial activities," *Surfaces and Interfaces*, vol. 17, Article ID 100359, 2019.

[50] S. Hameed, A. T. Khalil, M. Ali et al., "Greener synthesis of ZnO and Ag–ZnO nanoparticles using Silybum marianum for diverse biomedical applications," *Nanomedicine*, vol. 14, no. 6, pp. 655–673, 2019.

[51] D. Havenga, R. Akoba, L. Menzi et al., "From Himba indigenous knowledge to engineered Fe2O3 UV-blocking green nanocosmetics," *Scientific Reports*, vol. 12, no. 1, p. 2259, 2022.

[52] N. Ditlopo, N. Sintwa, S. Khamlich et al., "From Khoi-San indigenous knowledge to bioengineered CeO2 nanocrystals to exceptional UV-blocking green nanocosmetics," *Scientific Reports*, vol. 12, no. 1, p. 3468, 2022.

[53] A. Alnehia, A.-B. Al-Odayni, A. Al-Sharabi, A. H. Al-Hammadi, and W. S. Saeed, "Pomegranate peel extract–mediated green synthesis of ZnO-NPs: extract concentration-dependent structure, optical, and antibacterial activity," *Journal of Chemistry*, vol. 2022, Article ID 9647793, 11 pages, 2022.

[54] A. T. Khalil, M. Ovais, I. Ullah et al., "Bioinspired synthesis of pure massicot phase lead oxide nanoparticles and assessment of their biocompatibility, cytotoxicity and in-vitro biological properties," *Arabian Journal of Chemistry*, vol. 13, no. 1, pp. 916–931, 2020.

[55] W. Muhammad, N. Ullah, M. Haroon, and B. H. Abbasi, "Optical, morphological and biological analysis of zinc oxide nanoparticles (ZnO NPs) using Papaver somniferum L," *RSC Advances*, vol. 9, no. 51, pp. 29541–29548, 2019.